International Journal of
Nanotechnology and Allied Sciences
2017 | Volume 1 | Issue 1 | Pages 30-44
ISSN: 2523-9252 (Online)

www.psmpublishers.org

Research Article Open access

Elucidative Physiological Optimization of Silver Nanospheres Biogenesis by Molds

Amal, A.I. Mekawey, Eman A. Helmy

The Regional Center for Mycology and Biotechnology, Al-Azhar University, Cairo, Egypt.

Received: 31.Aug.2017; Accepted: 11.Nov.2017; Published: 23.Nov.2017
***Corresponding author: Eman A. Helmy; Email: dr_emanhelmy@azhar.edu.eg**

Abstract
One of the substantial and most ordinary requests asked for that when starting to oversee nanoparticles is "The reason is nanoparticles so intriguing? Why work with these to an incredible degree little structures that are attempting to manage and join especially when differentiated and their obviously noticeable accomplices? The suitable reaction lies in the novel properties controlled by these nanoparticles. *In vitro* myco synthesis of silver nanoparticles (AgNPs) using *Penicillium aurantiogresium, Penicillium roqueforti, Aspergillus niger, Verticillium chlamydosporium var. chlamydosporium, Trichoderma viride* and *Trichoderma longibranchiatum* had been investigated. The procedure of silver particle lessening by either extracellular contagious filtrate or intracellular without cell filtrate was accomplished which prompt the improvement of an easy procedure for the amalgamation of silver nanoparticles. Upon exposure of the fungal filtrate to silver nitrate, the latter was reduced to silver nanoparticles as indicated by a color change observed and characterized by UV-visible spectroscopy. The optimum experimental conditions for AgNPs synthesis were found to be a temperature of 37^{o}C at pH of 6.0 and a substrate concentration of 2mM silver nitrate after 24 hours incubation times in dark and measured spectrophotometrically at 430 nm. Silver nanoparticles created were described by different expository procedures, for example, TEM, FT-IR, and X-Ray investigation of both EDX and XRD. The acquired outcomes uncovered that the extent of nanoparticles for all the tried organisms extended from 8.97 to 16.73 nm with variable shapes, a generous portion of them exhibit in a circular nature.
Keywords: Silver Nanoparticles, Biosynthesis, Optimization, Fungi, Nanobiotechnology.

Cite this article: Mekawey, A.A.I., Helmy, E.A., 2017. Elucidative Physiological Optimization of Silver Nanospheres Biogenesis by Molds. Int. J. Nanotech. Allied. Sci., 1(1): 30-44.

INTRODUCTION

Nanotechnology gives a decent stage to change and build up the essential properties of metal as nanoparticles having promising applications in diagnostics, biomarkers, cell naming, differentiate operators for natural imaging, antimicrobial specialists, tranquilize conveyance frameworks and nano drugs for treatment of different illnesses (Marcato and Duran, 2008; Singh and Singh, 2011). The term nano is adjusted from the Greek word signifying "overshadow." When utilized as a prefix. Indeed, even the Greeks utilized it for cooking and to protect water. The principal recorded restorative utilization of silver was accounted for amid the eighth century it suggests 10-9. A nanometer (nm) is one billionth of a meter or generally the length of three particles one next to the other. A DNA atom is 2.5 nm wide, a protein roughly 50 nm, and an influenza infection around 100 nm. A human hair is roughly 10,000 nm thick. A nanoparticle is a tiny molecule with no less than one measurement under 100 nm (Li *et al.,* 1999). Exceptional properties of nanostructured materials qualify them for different applications, for example, sensor, hardware, optical gadgets and some more. Silver nanoparticles are broadly integrated and researched for optical and antimicrobial properties utilizing different strategies (Akinsiku *et al*., 2018).

Nanoparticles are of unbelievable legitimate eagerness as they vanquish any block between mass materials and atomic or nuclear structures. A mass material has enduring physical properties paying little regard to its size, be that as it may, at the nanoscale, this is much of the time not the circumstance. A couple of all around depicted mass materials have been found to have most captivating properties when analyzed at the nanoscale. There are many purposes behind this including the way that nanoparticles have a high point of view extent. The exceptional excitement for respectable metal has been taken since they don't encounter disintegration or oxidation successfully (Zhao and Stevens, 1998). Metallic nano-materials have pulled in consideration as a result of their one of a kind organic and physicochemical properties contrasted with their large scale partners. Gold, silver and

copper nanoparticles show solid ingestion of electromagnetic waves in the obvious range because of Surface Plasmon Resonance (SPR) which is very impacted by shape and size of the nanoparticles (Zhao and Stevens, 1998). In this way, they stable scatterings of nanoparticles are helpful in zones, for example, microbiology, medicinal conclusion, photography, catalysis, natural naming, photonics and optoelectronics, gadgets, beautifiers, coatings, bundling, and biotechnology.

Silver nanoparticles (AgNPs) are generally being utilized on the grounds that it is more powerful against bacteria's. In the blend of AgNPs, the preparing condition should be controlled in such a way, to the point that the subsequent nanoparticles have an indistinguishable shape, indistinguishable size, and exclusively scattered with no agglomeration (Banerjee *et al.,* 2014). AgNPs are generally favored for biomedical applications on the grounds that; Ag+ particles are exceedingly perfect for the human body. Numerous strategies have been accounted for the blend of AgNPs (Nia *et al.*, 2015), yet just a couple of techniques have created a size controlled and monodispersed AgNPs. These monodispersed AgNPs greatly affect their physical and concoction properties. Every one of the techniques have focused on getting ready particles of little size and unmistakable shape which centers for various applications (Solomon and Umoren, 2016).

Ordinarily, nanoparticles have a wavelength beneath the basic wavelength of light. This renders them straightforward, a property that makes them exceptionally helpful for applications in makeup, coatings, and bundling (Cohen *et al.,* 2007). AgNPs has been known as superb calming operator, and along these lines were utilized to enhance wound mending (Elliott, 2010). Silver nanoparticles are of enthusiasm for applications in therapeutic gadgets and medicinal services items because of their antibacterial action and low harmfulness to human's cells. In this manner, reactants utilized as a part of the nanoparticle amalgamation ought not be poisonous or aggravation. The alleged "green combination" strategies suit well these reasons. "Green amalgamation" of nanoparticles makes utilization of ecologically neighborly, non-dangerous and safe reagents (Kilin *et al.,* 2008).

Contrasted and the customary manufactured strategies, organic frameworks give an original plan to the generation of nano-materials. Up to now, a few microorganisms from microscopic organisms to parasites have been accounted for to combine inorganic materials either intra-or additional cell, and along these lines to be conceivably used as eco-accommodating. Microbes are known to improve particles and orchestrate magnetite gems and to change over metals into nanoparticles of silver and gold. Organisms have been known to discharge significantly higher measures of bioactive substances, which made parasites more appropriate for huge scale. Furthermore, the extracellular biosynthesis utilizing parasites could likewise make downstream handling considerably simpler than microscopic organisms creation (Bharde *et al.,* 2006). An intriguing case of the biosynthesis utilizing parasites was that the cell-related biosynthesis of silver utilizing *Fusarium oxysporum* was exhibited by Ahmad *et al.,* (2003b). Past reports have demonstrated that numerous dynamic substances discharged by growths including catalysts which assumed essential parts in decreasing specialists and topping operators in the response (Bharde *et al.,* 2006).

Hence, it was of incredible criticalness to investigate novel parasites strain for integrating AgNPs in view of the biodiversity. Accordingly, the natural approach for the amalgamation of nanoparticles winds up noticeably vital. An immense range of organic assets accessible in nature including plants and plant items, green growth, parasites, yeast, microorganisms, and infections could all be utilized for blend of nanoparticles. Of note, both unicellular and multicellular living beings have been known to deliver intracellular or extracellular inorganic materials (Kuber *et al.,* 2006). Despite these noteworthy outcomes, the roots of organisms having the capacity for AgNPs union were yet constrained, and the definite instrument was yet not all around clarified.

Consequently, the present investigation was embraced to screen the capacity of six contagious concentrates to lessen fluid silver nitrate to silver nanoparticles, additionally improvement conditions for biosynthesis of silver nanoparticles e.g., temperature, pH, hatching period and the best grouping of silver nitrate were acquired. At last; describing the silver nanoparticles utilizing TEM; X-Ray examination of both EDX and XRD and Fourier change infrared (FTIR) were broke down.

MATERIALS AND METHODS

Microorganisms

Six parasitic disconnects: *Penicillium aurantiogresium* (IMI 89372); *P. roqueforti* (IMI 285518); *Aspergillus niger* (NRRL 595); *Verticillium chlamydosporium var. chlamydosporium* (CBS 600.88); *Trichoderma viride* (RCMB 004001); and *T. longibranchiatum* (RCMB 004006) were benevolently given from the way of life accumulation unit of the Regional Center for Mycology and Biotechnology (RCMB) Al-Azhar University, Cairo-Egypt. All parasitic separates were sub-refined and kept up on Sabouraud's Glucose agar (SGA) medium containing (g/l); glucose– 20; peptone– 10; agar– 20 and refined water,1000 ml; pH of medium was changed in accordance with 5.4 ± 0.2 at 25 (±2) °C.

Biomass production

To get ready biomass for biosynthesis ponders, the parasite was developed vigorously in a fluid media containing (g/l) $KH2PO_4$– 7.0; K_2HPO_4– 2.0; $MgSO_4$– 0.1; $(NH_4)_2SO_4$– 1.0; yeast extract– 0.6; and glucose– 10.0. pH (6.2 ± 0.2). The carafes were vaccinated and hatched on an orbital shaker at 25°C and unsettled at 150 rpm. The

biomass was collected after 72 h of development by sieving through Whatmann channel paper no.1 took after by broad washing with refined water to expel any medium segment from the biomass according to Kathiresan et al. (2009).

Extraction of intra and extracellular extract for biosynthesis of AgNPs

To plan extracellular contagious biosynthesis of AgNPs, 20 g of crisp clean biomass was gotten contact with 100 ml of deionized water in an Erlenmeyer carafe and brooded at 25°C in dull shaking hatchery (150 rpm) for 72 h. After brooding, the cell filtrate was acquired by doing it through Whatmann channel paper no.1. For the blend of silver nanoparticles, 50 ml $AgNO_3$ (1mM) was blended with 50 ml of extracellular contagious filtrate in a 250 ml Erlenmeyer jar and unsettled at 25◦C and pH 4.0 in dim shaking hatchery at 150 rpm for 72 h. Ordinarily, to plan intracellular biosynthesis of AgNPs, 20g (wet weight) test of contagious mycelia were upset utilizing homogenizer and deionized sanitized water, to discharge the intracellular sans cell remove into the fluid arrangement. The sans cell separates blended with 100 ml deionized sanitized water and brooded at 25°C and pH 4.0 in dim shaking hatchery at 150 rpm for 72 h. The carafe substance was separated by Whatman no. 1 channel paper. Filtrates were along these lines utilized for the biosynthesis of AgNPs. At that point, 50 ml of the without cell separate was blended with 50 ml of 1 mM of $AgNO_3$ and unsettled in an indistinguishable condition from depicted before. Two Controls were utilized; first negative control containing just biomass without the silver particle, and the second positive control containing 1mM $AgNO_3$ that keep running alongside the trial cups according to Kathiresan et al. (2009).

UV–visible spectrophotometeric analysis

The lessening of silver particles was affirmed by subjective testing of supernatant by UV– unmistakable spectrophotometer (Spectronic Milton Roy 1201 UV). 1mM of $AgNO_3$ was blended with 50 ml of cell filtrate in a 250 ml Erlenmeyer flagon at 25oC and pH 4 and disturbed in dull. Optical thickness was estimation every 10 min from the earliest starting point of hatching until 72 hands at the diverse wavelength extending from 200 to 800 nm and plotted the qualities on a diagram (to decide the best time for brooding and the best wavelength recognizing AgNPs blend).

Optimization of physic–chemical parameters for biosynthesis of nanoparticles

Impact of temperature, pH and hatching times on the creation of silver nanoparticle was improved by changing the parameters each one in turn, for example, substrate fixation (0, 1, 2, 3, 4, 5, 6, 7, 8, 9, 10 mM of AgNO3), temperature (5, 20, 28, 37, 50, 75 ◦C) and pH (1, 2, 3, 4, 5, 6, 7, 8, 9, 10). The example of 1ml was pulled back at various time interims and the optical absorbance was measured at the best wavelength which decided already.

Purification of AgNPs

The dry powders of each AgNPs were gotten by the accompanying way: after wanted response period, the juices containing silver nanoparticles was centrifuged at 10,000 rpm for 15 min, following which the pellet was re-scattered in sterile refined water to dispose of any clumsy organic particles. The procedure of centrifugation and re-scattering in sterile refined water was rehashed three times to guarantee better division of free elements from the metal nanoparticles. The sanitized pellets were then sonicated for 30 min utilizing ultrasonicator (joined Jeveriy instruments supplies, Italy) for greater dissimilarity. At long last, specimens were solidifying dried utilizing a lyophilizer (Thermo Electron Corporation, Micro Modulyo 230 stop dryer) according to Tripathy et al. (2010).

Partial purification and SDS-PAGE analysis

For partial protein purification and sodium dodecyl sulphate polyacrylamide gel electrophoresis (SDS-PAGE) performance of the purified protein, the optimal concentration of $AgNO_3$ was mixed with 50 ml of cell filtrate in a 250 ml Erlenmeyer flask and agitated in dark as earlier conditions according to Kathiresan et al., (2009). Then after 24 h, the cell supernatant was hastened by tenderly blended for overnight with strong ammonium sulfate to 80% immersion at 4◦C. The pellet got after centrifugation was broken down in 0.05M phosphate support (pH 8.0). The protein focus was resolved per Lowery *et al.,* (1951). The came about protein was dialyzed overnight against 0.05M phosphate cradle (pH 8.0) to expel overabundance salt. Cleaned tests were investigated on sodium dodecyl sulfate-polyacrylamide gel electrophoresis (SDS-PAGE) per Hames and Rickwood (1990) to check the virtue and to decide the sub-atomic weight of the refined protein groups by contrasting and standard protein marker having the sub-atomic weight running from 10 to 250 kDa. Electrophoresis was performed utilizing Bio-Rad Mini-Protean gel framework at a steady voltage of 100 kV for 120 min. After electrophoresis, the gel was recolored with Coomassie Brilliant Blue color and was seen in a gel imaging framework (Bio-Rad, USA). To explore the proteins which are bound to the surface of silver nanoparticles, tests were overflowed with 1% SDS answer for 10 min took after by centrifugation at 8000 rpm for 10 min for the gathering of the supernatant. The SDS-treated and untreated specimens were additionally examined by the 12% SDS-PAGE as portrayed prior.

Characterization of the biosynthesized silver nanoparticles

The portrayal of silver nanoparticles was done by various instruments and procedures. It incorporates visual perception, UV– Visible spectrophotometer, X-beam

diffraction (XRD) of TEM, vitality dispersive X-beam (EDX) of SEM, Fourier change infrared (FT-IR) investigation and TEM. Likewise, incomplete protein purging and sodium dodecyl sulfate-polyacrylamide gel electrophoresis (SDS-PAGE) of the filtered protein and in addition nanoparticles focuses were resolved.

Transmission Electron Microscopy (TEM) Analysis

Silver nanoparticles measure width and shape, and in addition, the impact of pH and temperature degrees on AgNPs highlights (shape and size), were accounted for and dictated by Transmission Electron Microscopy (TEM JEOL 1010, Japan) and X-beam diffraction (XRD) of (XRD/TEM JEOL 1010, Japan). Tests for TEM were set up by setting a drop of AgNPs arrangement onto an ordinary carbon-covered copper TEM networks (400 lattices, Plano Gmbh, Germany), enabling the drop to dry overnight at room temperature before imaging. X-beam diffraction investigations, and the TEM pictures of the examples, were gotten utilizing a quickening voltage of 30 kV and 80 kV, separately. No less than three pictures of each specimen were taken to have an unmistakable portrayal of its morphology.

Scanning Electron Microscope (SEM) Analysis

For SEM imaging, a sample of a solution was placed on a carbon strip attached to a SEM brass support and dried at 50°C for 5 min. The energy-dispersive X-ray (EDX) spectra (SEM/EDX, JSM-5500 LV JEOL, SEM, Japan) were used to examine the dimension, morphology, and chemical composition of the samples. Surface binding elements were analyzed with X-ray photoelectron spectroscopy. Silver nanoparticle which was excited by an electron beam showed the peak values of Ag element.

Fourier Transform Infra-Red (FT-IR) Spectroscopy analysis

The infrared analysis of the nanoparticles was performed on a Fourier transform infrared (FT-IR) spectrometer (IRPrestige-21®, German) to understand the protein–nanoparticle interaction and to identify the possible biomolecules which are responsible for reduction of Ag^+ ion and capping of the bio-reduced nanoparticles synthesized by the fungal cells. Prior to analysis, the fungal filtrate containing nanoparticles was stirred at speed of 5,000 rpm for 10 min, and it was then washed with deionized water three times and air-dried. The dried samples were pressed into pellets. The sample pellets were placed into the sample holder and FT-IR spectra were recorded in the range of 450–4,000 cm^{-1} at a resolution of 4 cm^{-1}.

Determination of nanoparticle concentration

Accurate determination of the size and concentration of nanoparticles is essential for the biomedical application of nanoparticles. The concentration of AgNPs to be administered at the level was determined by a method which has been previously reported. The calculation was as follows: Initially the average number of atoms per nanoparticles was calculated using the formula described by Sriram et al. (2010).

$$N = \frac{\pi \rho D^3}{6\,M} NA$$

Where N = number of atoms per nanoparticle, π = 3.14, ρ = density of face-centered cubic silver = 10.5g/cm^3, D = average diameter of nanoparticles = 50 nm = 50 × 10−7 cm, M = atomic mass of silver = 107.868 g, N_A = number of atoms per mole (Avogadro's number = 6.023 × 10^{23}).

Therefore, assuming 100% conversion of all silver ions to silver nanoparticles:

$$N = \frac{(\pi \text{ X } 10.5 \text{ X } (50.0 \text{ X } 10^{-7})^3 \text{X } 6.023 \text{ X } 10^{23})}{6 \text{ X } 107.868}$$

i.e., *N* =3837233.003, then the molar concentration of the nanoparticle solution was determined by:

$$C = \frac{N_T}{NVN_A}$$

Where; *C* =molar concentration of the nanoparticle solution, *N*T =total number of silver atoms added as AgNo3 =1 M, *N* =number of atoms per nanoparticle (from above calculation), V =volume of the reaction solution in L, NA =Avogadro's number (6.023 ×10^{23})

$$C = \frac{[1\text{X}6.023\text{X}10^{23}]}{3837233.003\text{X}1\text{X}6.023 \text{ X } 10^{23}}$$

Where; C =2.606 X10^{-7}, M/L =2600 nM/10 mL.

The required concentrations were thereafter made up from the obtained values.

RESULTS AND DISCUSSION

Investigation of extracellular and intracellular biosynthesis of silver nanoparticles by six contagious species was done along this work. The parasitic biomass after hatching for 72h with disinfected deionized refined water was isolated by filtration. The cell of both additional and intra filtrates hatched with silver particle toward the start of the response. The cups being hatched oblivious in an ecological shaker indicated the steady change in shade of the medium to darker, with force expanding amid the time of brooding. The outcome demonstrated union of silver nanoparticles of silver particles meeting the filtrate **(**Figure 1).

The change in color of the medium was noted by visual observation. The solution remained as hydrosol and no precipitation was observed. Control (without silver particle) demonstrated no adjustment in shade of the cell filtrate when brooded in the same natural condition. The present outcomes uncovered that all contagious disconnects shaped nanoparticles with silver nitrate in both additional and intracellular filtrates aside from *Aspergillus niger* and *Verticillium chlamydosporium var. chlamydosporium* framed nano-silver particles just in intracellular filtrates (Table 1).

Table 1. Biosynthesis of AgNPs by fungal filtrates, (+) AgNPs formation; (-) AgNps not observed

	Extra cellular filtrate	Intra cellular filtrate
Penicillium aurantiogresium	+	+
Penicillium aurantiogresium	+	+
P. roqueforti	+	+
Aspergillus niger	-	+
Verticillium chlamydosporium var. *chlamydosporium*	-	+
Trichoderma viride	+	+
T. longibranchiatum	+	+

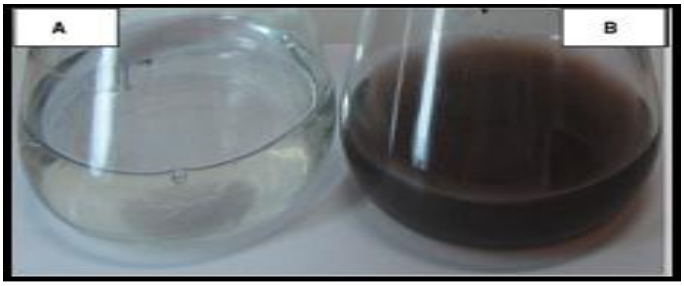

Fig. 1. Culture filtrate with silver ions: (A): at the beginning of reaction and (B): after 72 h of reaction

Many reports in concurrence with these outcomes, for example, Ahmad *et al.,* (2003 a) who watched that it was watched endless supply of the silver particle (1 mM) into the carafe containing the cell filtrate of *Fusarium oxysporum,* the shade of the medium changed quickly to dark colored. The presence of the darker shading meant that the arrangement of colloidal silver nanoparticles in the medium. Likewise, Kuber *et al.,* (2006) have demonstrated the extracellular amalgamation of silver nanoparticles inside hours of contact time. The expansion in power could be because of expanding number of nanoparticles framed in view of decrease of silver particles introduce in the watery arrangement.

The present examination uncovered that silver nanoparticle blend regarding shading power of culture filtrates was analyzed at various wavelengths and hatching times. The retention range of the medium containing the silver particles was measured from 200 to 800 nm and the best time of hatching was determinate at every 10 min. until 27 h. the outcomes demonstrated expanded retention power near 400 and 500 nm with the goal that optical thickness was estimation every 10 min at the distinctive wavelength running from 400 to 500 nm to determinate precisely the best wavelength. A look at 430 nm was the best wavelength of the ultra violet beam to the estimation of AgNPs in all filtrates (Table 2), additionally, Table (3) revealed 24h hatching time was the best time of brooding.

These outcomes concur with Ahmad *et al.,* (2003b) who detailed that silver nanoparticles with great mono-dispersity have been accounted for by utilizing *Thermonospora* sp. The nanoparticles introduce in the watery medium were very steady, even up to 4 months of hatching at 25 °C. the way that silver nanoparticles top stayed near 430 nm even after 72 h of brooding demonstrates that the particles were all around scattered in the arrangement and there was very little accumulation.

Presently, silver nitrate (substrate) focus (0– 10 mM); temperature (5, 20, 28, 37, 50 and 75◦C); pH (1– 10) were concentrated to determinate the ideal condition for biosynthesis of nanoparticles at 430 nm and after 24h hatching. The outcomes announced that the absorbance spectra showed the best $AgNO_3$ fixation utilized for biosynthesis of AgNPs was 2.0 mM (Table 4), and the best temperature and pH were 37 ◦C (Table 5) and pH 6.0 (Table 6).

Hayat (1990) uncovered that combination of silver and gold nanoparticles utilizing microscopic organisms and parasites, the time required for the finish of the response ranges from 60 to 120 h, while the 24 h brooding showed the greatest amalgamation of silver nanoparticles. The metal gathering is reliant on the development period of cells. While Kathiresan *et al.,* (2009) recorded that, nanoparticle union as far as shading force of culture filtrate of *Penicillium fellutanum* was inspected at various wavelengths, pH, hatching time, temperature and silver nitrate focus. The absorbance spectra displayed a crest at 430 nm. At this wavelength, the most astounding optical thickness was found at 24 h of brooding time, pH 6.0, the temperature of 5◦C and 1.0mM convergence of silver nitrate.

Table 2. Different UV–visible spectrum (nm) of aqueous medium containing cell filtrates directly after mixed with silver nitrate (1 mM) after 72 incubation times (E): extracellular ; (I): intracellular : (-): not obtained

UV Optical density	*P. aurant*		*P. roquef*		*A. nige*		*V.chlamy.*		*T. viride*		*T. long*	
	E	I	E	I	E	I	E	I	E	I	E	I
200	-0.09	-1.03	-0.75	-1.45	-	-1.35	-	-1.21	-0.23	-0.81	-0.06	-0.47
300	1.05	1.02	1.05	1.02	-	1.14	-	1.26	1.01	1.37	0.22	0.39
400	1.09	1.26	1.15	1.27	-	1.38	-	1.48	1.31	1.70	0.77	0.88
410	1.13	1.98	1.23	1.57	-	1.20	-	1.57	1.42	1.76	0.75	1.58
420	1.18	2.16	1.20	1.94	-	1.22	-	1.87	1.55	1.86	0.74	1.78

Table 3. UV–visible spectrum at 430 nm of aqueous medium containing cell filtrates and silver nitrates (1 mM) at different incubation times

Incuba-tion times	*P. aurant*		*P. roquef*		*A. nige*		*V.chlamy.*		*T. viride*		*T. long*	
	E	I	E	I	E	I	E	I	E	I	E	I
10 min	1.34	1.45	1.19	1.08	-	1.15	-	0.93	2.12	1.08	1.58	1.14
20 min	1.49	1.55	1.32	1.25	-	1.22	-	1.03	2.16	1.14	1.72	1.20
30 min	1.55	1.64	1.44	1.35	-	1.25	-	1.17	2.23	1.37	1.86	1.36
40 min	1.65	177	1.50	1.57	-	1.40	-	1.30	2.34	1.46	1.92	1.42
50 min	1.72	1.83	1.54	1.66	-	1.99	-	1.85	2.38	1.51	1.98	2.50
60 min	1.76	2.28	1.61	1.95	-	2.04	-	2.26	2.36	1.65	2.02	2.54
120 min	1.78	2.32	1.66	2.09	-	2.35	-	2.38	2.39	1.73	2.19	2.60
180 min	1.62	2.48	1.75	2.66	-	2.49	-	2.40	2.42	1.85	2.34	2.74
24 hrs	**1.86**	**2.69**	**2.29**	**2.88**	**-**	**2.94**	**-**	**2.54**	**2.56**	**2.35**	**2.52**	**2.95**
48 hrs	1.77	2.32	2.12	2.65	-	2.43	-	2.30	2.32	2.15	2.49	2.86
72 hrs	1.49	2.29	1.97	2.52	-	2.37	-	2.17	1.79	2.08	2.39	2.61

(E): extracellular ; (I): intracellular : (-): not obtained

Table 4. UV–visible spectrum at 430 nm of aqueous medium containing cell filtrates and different concentrations of silver nitrates after 24hrs at 25 °C and pH 4.0.

$AgNO_3$ Conc.	*P. aurant*		*P. roquef*		*A. niger*		*V. chlamy*		*T. virid*		*T. long*	
	E	I	E	I	E	I	E	I	E	I	E	I
0mM	0.24	1.01	0.45	1.59	-	1.48	-	0.12	0.27	1.18	0.16	0.27
1 mM	1.86	2.69	2.29	2.88	-	2.94	-	2.54	2.56	2.35	2.52	2.95
2 mM	**2.21**	**2.96**	**2.54**	**3.27**	**-**	**3.12**	**-**	**2.95**	**2.63**	**2.52**	**2.84**	**3.42**
3 mM	1.98	2.82	2.02	2.81	-	2.88	-	2.62	2.41	2.38	2.60	3.06
4 mM	0.86	2.73	1.75	2.50	-	2.65	-	2.58	1.83	2.22	2.08	2.65
5 mM	0.99	2.69	1.54	2.46	-	2.50	-	2.42	1.71	2.12	1.49	2.41
6 mM	1.03	2.56	1.49	2.08	-	2.38	-	1.82	1.70	1.90	1.22	2.02
7 mM	1.12	2.43	0.91	1.99	-	2.18	-	1.68	1.09	1.52	0.83	1.45
8 mM	1.37	2.33	0.72	1.96	-	1.40	-	1.00	0.83	1.46	0.52	1.36
9 mM	1.67	2.16	0.76	1.95	-	1.31	-	0.93	0.58	1.38	0.28	1.28
10 mM	0.92	2.14	0.66	1.88	-	0.96	-	0.78	0.41	1.25	0.11	1.11

(E): extracellular ; (I): intracellular : (-): not obtained

Table 5. UV–visible spectrum at 430 nm of aqueous medium containing cell filtrates and silver nitrates (2 mM) after 24hrs at different temperatures and pH 4.0.

Temp.	*P. aurant*		*P. roquef*		*A. nige*		*V.chlamy.*		*T. viride*		*T. long*	
	E	I	E	I	E	I	E	I	E	I	E	I
5 °C	1.21	2.34	1.05	2.58	-	2.70	-	1.18	2.02	2.60	2.13	2.00
20 °C	1.66	2.55	1.97	3.06	-	3.03	-	1.90	2.16	3.47	2.36	2.40
28 °C	2.11	2. 86	2.04	3.67	-	3.98	-	2.25	**2.23**	3.82	2.64	3.22
37 °C	**2.33**	**3.31**	**2.48**	**4.41**	**-**	**4.36**	**-**	**2.63**	2.09	**4.41**	**3.66**	**3.96**
50 °C	1.82	2.40	1.86	3.95	-	3.51	-	2.45	1.24	4.00	2.51	3.10
75 °C	1.37	0.22	0.36	1.83	-	2.14	-	1.06	0.20	2.23	1.35	1.28

(E): extracellular ; (I): intracellular : (-): not obtained

Table 6. UV–visible spectrum at 430 nm of aqueous medium containing cell filtrates and silver nitrates (2 mM) and 37°C after 24hrs at different pH

pH	*P. aurant*		*P. roquef*		*A. nige*		*V.chlamy.*		*T. viride*		*T. long*	
	E	I	E	I	E	I	E	I	E	I	E	I
1	1.89	2.31	2.15	2.21	-	2.46	-	1.25	1.26	2.15	2.96	3.56
2	2.35	2.56	2.36	2.89	-	3.15	-	1.89	1.75	2.89	3.28	4.59
3	3.56	2.79	2.75	3.14	-	3.48	-	2.00	2.01	3.25	3.95	5.62
4	4.15	2.90	2.81	3.67	-	3.96	-	2.12	2.45	4.56	4.56	6.15
5	4.63	3.21	3.28	4.11	-	4.06	-	3.33	3.39	5.21	5.46	6.76
6	**5.06**	**5.26**	**4.86**	**6.99**	**-**	**6.90**	**-**	**5.46**	**4.46**	**6.32**	**6.97**	**7.65**
7	3.64	4.42	3.65	4.82	-	5.83	-	4.25	3.93	5.18	5.89	5.55
8	2.09	3.16	2.64	3.76	-	4.79	-	3.16	2.32	4.80	4.67	3.42
9	1.94	2.83	1.55	2.65	-	3.72	-	2.52	1.22	3.76	3.45	2.38
10	1.52	1.49	0.46	1.60	-	1.68	-	1.20	0.19	2.73	2.12	1.96

(E): extracellular ; (I): intracellular : (-): not obtained

TEM micrograph of silver nanoparticles was acquired in the present research at 25oC and pH 4 as control (straightforwardly from parasitic sifted) and in 37oC and pH 6.0 as ideal conditions for the AgNPs biosynthesis process. The pictures of the AgNPs comes about are appeared in the Figure (2). The immediate electron infinitesimal representation permits measuring the size and state of the silver nanoparticles shaped. The micrograph demonstrated nanoparticles with variable shape, most them show in the circular in nature (a substantial portion of the silver nanoparticle utilized) (Figure, 2"A"). The measure of the nanoparticles from all contagious sifted utilized as a part of extended from 8.17 to 16.73 nm, additionally, Conc. of particles per AgNPs (M/ L) were identified (Table 7 and Figure 3). The sizes of AgNPs were modified extraordinarily at the temperature of 37oC and pH of 6.0 (Figure, 2"B") with some having every so often barrel-shaped or triangular shape (as nanoparticles from *T. viride* extracellular concentrate) (Figure, 2"C"). The larger part of the silver nanoparticles were scattered with just a couple of them indicating totals (as nanoparticles from *A.niger* intercellular concentrate) of differing sizes as saw under TEM (Figure, 2" D").

Table 7. Mean of diameters of the sizes (nm) and concentration of AgNPs (M/L) at normal phase and under optimal conditions

		P. aurant		*P. roquef*		*A. nige*		*V.chlamy.*		*T. viride*		*T. long*	
		E	I	E	I	E	I	E	I	E	I	E	I
Mean of Sizes of AgNPs (nm)	*Cont*	12.70	16.73	15.13	11.70	-	14.48	-	8.97	13.47	12.86	11.00	12.95
	Temp	9.89	13.27	9.43	11.57	-	11.30,	-	12.23	9.91	10.77	8.17	10.39
	pH	8.99	10.92	8.53	16.33	-	11.26	-	11.98	10.54	9.75	8.60	11.81
Conc. of atoms per AgNPs (M/L)	*Cont*	$3.1818X\ 10^{-5}$	$1.3918\ X\ 10^{-5}$	$1.8818X\ 10^{-5}$	$4.069\ X\ 10^{-5}$	-	$2.146\ X\ 10^{-5}$	-	$8.970\ X\ 10^{-5}$	$2.6668X\ 10^{-5}$	$3.0011\ X\ 10^{-5}$	$489.6\ X\ 10^{-5}$	$3.0011\ X\ 10^{-5}$
	Temp	$6.696\ X\ 10^{-5}$	$278.9\ X\ 10^{-5}$	$7.772\ X\ 10^{-5}$	$420.81\ X\ 10^{-5}$	-	$451.7\ X\ 10^{-5}$	-	$3.56\ X\ 10^{-5}$	$6.696\ X\ 10^{-5}$	$521.73\ X\ 10^{-5}$	$1.195\ X\ 10^{-5}$	$581.10\ X\ 10^{-5}$
	pH	$8.970\ X\ 10^{-5}$	$500.52\ X\ 10^{-5}$	$1.050\ X\ 10^{-4}$	$149.67\ X\ 10^{-5}$	-	$456.54\ X\ 10^{-5}$	-	$379.07\ X\ 10^{-5}$	$5.566\ X\ 10^{-5}$	$703.20\ X\ 10^{-5}$	$1.024\ X\ 10^{-4}$	$395.68\ X\ 10^{-5}$

(E): extracellular ; (I): intracellular : (-): not obtained

Numerous prior reports affirm our outcomes, for example, Duran *et al.,* 2005; Kuber *et al.,* (2006) and Kathiresan *et al.,* (2009) who got that TEM picture of nanoparticles demonstrates singular silver nanoparticles incorporated by *F. oxysporum* and *Penicillium* strain and various totals. The morphology of the nanoparticles is exceedingly factor. Under perception of such pictures, these gatherings were observed to be totals of silver nanoparticles in the size range 5– 50 nm. The nanoparticles were not in coordinate contact even inside the totals. The division between the silver nanoparticles found in the TEM picture could be because of topping by proteins and would clarify the UV-Vis spectroscopy estimations, which is normal for all around scattered silver nanoparticles. The silver nanoparticles are crystalline, as can be seen from the chosen region diffraction design recorded from one of the

nanoparticles in the totals. And, Mohammed *et al.,* (2009) revealed that in TEM micrograph demonstrates silver nanoparticles combined at 27 ◦C indicates circular and occasionally bar like silver nanoparticles ranges from the measure of 10– 40 nm. In the lower temperature of 10 °C, demonstrates the arrangement of silver nanoplates and the size extents from 80 to 100 nm, they watch the expansion in response temperature comes about abatement in molecule estimate, while the diminishing in response temperature comes about increments in molecule measure. The diminishing in molecule size and restricted size appropriation with the expansion in temperature is a notable wonder. It is regularly because of expanded response rate at the higher temperature.

As response rate is expanded the reactants devour speedier, henceforth reactant consumption happens, prompting the development of littler nanoparticles and limited size circulation at the higher temperature. Parasites are exceptionally outstanding to discharge countless which assume a key part in their life cycle. Most of these proteins incorporate hydrolytic compounds, for example, amylases, cellulases, and proteases (Jain *et al.,* 2010). A substantial portion of the proteomic ponders have concentrated on the proteins engaged with the metabolic pathways, be that as it may, different proteins and their part stay obscure. To distinguish the parasitic proteins in charge of the blend of silver nanoparticles, the sans cell filtrate was salted out overnight at 4 ◦C utilizing ammonium sulfate precipitation technique took after by centrifugation. The pellet division was thusly dialyzed utilizing a 10 to 250kDa cut-off film. The protein profiles were thought about by one dimensional SDS-PAGE took after by Coomassie Brilliant Blue recoloring (Figure 4 and Table 8). The protein divisions obviously demonstrated the nearness of two extraordinary groups in each parasitic concentrate utilized changes from 30 to 80kD in connection to each contagious protein sort. These proteins can oversee the union and the solidness of silver nanoparticles. Correspondingly, Ahmed *et al.,* (2003a) contemplate indicated two extracellular proteins utilizing *Fusarium oxysporum* having the atomic weight of 24 and 28 kDa in charge of the combination and adjustment of zirconia nanoparticles.

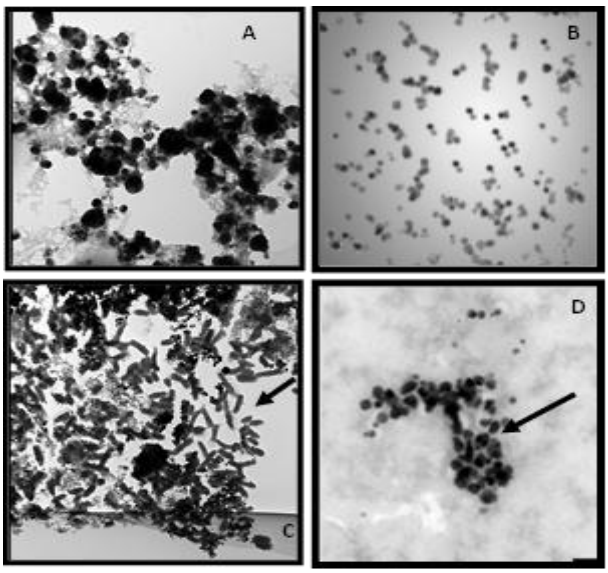

Fig. 2. TEM micrograph of synthesized silver nano particles (scale bar: 50 nm) from tested fungal extracts.
- (A): Control, nano particles at 25°C and pH 4 (directly from all fungal filtered used) the photo show spherical nanoparticles.
- (B): silver nano particles at 37°C and pH 6, the photo showed the spherical nanoparticles became smaller than control (from all fungal filtered used except *A.niger* and *T. viride*).
- (C): silver nano particles at 37°C and pH 6, the photo showed the cylindrical or triangular from *T.viride* extra cellular extract (arrow). shape nanoparticles (arrow).
- (D*): silver nano particles at 37°C and pH 6, the photo showed aggregation of nanoparticles from *A. niger* intracellular extract (arrow).

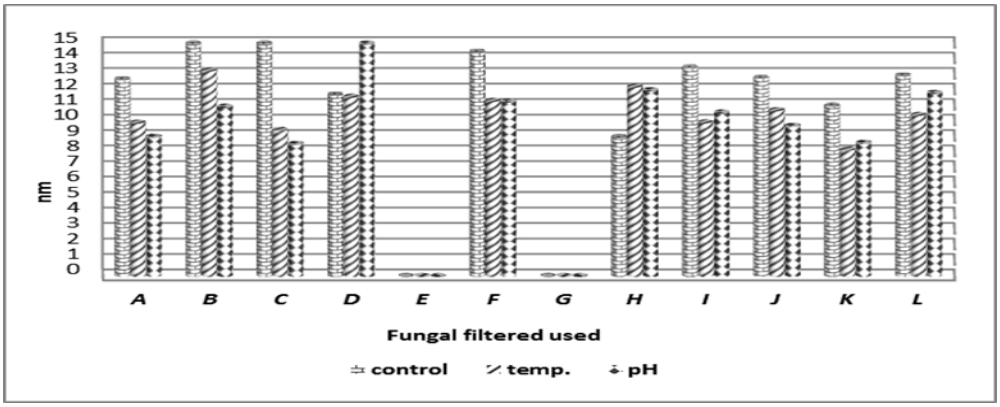

Fig. 3. The nanoparticle size distribution histogram obtained; (A): extracellular of *P. aurant.;*(B): intracellular of *P. aurant.*; (C): extracellular of *P. roquef.;* (D) : intracellular of *P. roquef.;* (E): extracellular of *A. niger.;*(F): intracellular of *A. niger;* (G): extracellular of *V.chlamy.*; (H): intracellular of *V.chlamy.*; (I): extracellular of *T. viride;* (J) : intracellular of *T. viride;* (K): extracellular of *T. long.;* (L) : intracellular

Table 8. molecular weight of the purified protein bands responsible for the synthesis and stabilization of Nanoparticles from fungal extracts

Fungal Extracts **Protein Bands (KDa)**	**A**	**B**	**C**	**D**	**E**	**F**	**G**	**H**	**I**	**J**
First protein band	**75**	**73**	**77**	**76**	**54**	**75**	**68**	**65**	**67**	**64**
Second protein band	**72**	**70**	**75**	**74**	**51**	**73**	**65**	**62**	**64**	**61**

(A): extracellular of *P. aurant*.; (B): intracellular of *P. aurant*.; (C): extracellular of *P. roquef*.; (D) : intracellular of *P. roquef*.; (E): intracellular of *A. niger*.; (F): intracellular of *V.chlamy*.; (G): extracellular of T. *viride*; (H) : intracellular of *T. viride*; (I): extracellular of *T. long*.; (J) : intracellular of *T. long*.

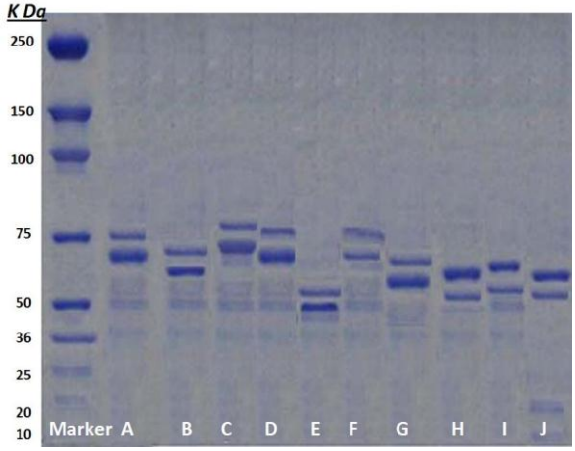

Fig. 4. SDS-PAGE patterns of purified protein of silver nitrate added culture filtrate. SDS-PAGE carried out using 10% polyacrylamide gel electrophoresis. Lane Marker; 250 KDa molecular weight marker; lanes A – J; purified protein from silver nitrate added culture of (A) extracellular of *P. aurant*.; (B) intracellular of *P. aurant*.; (C) extracellular of *P. roquef*.; (D) intracellular of *P. roquef*.; (E) intracellular of *A. niger*.; (F) intracellular of *V.chlamy*.; (G) extracellular of T. *viride*; (H) intracellular of *T. viride*; (I) extracellular of *T. long*.; (J) intracellular of *T. long*. Two bands at each fungal extract were observed.

The system for the union of silver nanoparticles is conjectured. The combination procedure happens in two stages: right off the bat, lessening of mass silver particles into silver nanoparticles and, besides, topping of the as-orchestrated nanoparticles. The initial step includes a first band protein which might be a reductase discharged by the parasitic separate, which might be for diminishment of silver particles into silver nanoparticles. The second step includes second band proteins which tie with nanoparticles and give soundness. The protein– nanoparticle associations can assume an exceptionally critical part in giving soundness to nanoparticles. Hard works are continuous to dispose of polluting influences and separate these two proteins.

As a stage towards understanding the instrument of silver nanoparticles, the protein profile of the without cell filtrate was investigated. SDS-PAGE profiles of the extracellular proteins in charge of the amalgamation and strength (topping operator) of silver nanoparticles utilizing the organism Aspergillus flavus NJP08 by Jain *et al.,* (2010) demonstrated the nearness of two extreme groups of 32 and 35 kDa which oversee the union and soundness of silver nanoparticles, individually. This report demonstrating a huge investigation on the proteins bound to nanoparticle surface promptly upon contact with the nanoparticles. The protein adsorption has been generally contemplated, and it has been discovered that protein adsorption relies upon numerous factors, for example, electrostatic, hydrophobic and synthetic associations between the protein and the adsorbent.

Ahmad *et al.,* (2003 a) have revealed that specific NADH subordinate reductase was associated with the diminishment of silver particles in the event of *F. oxysporum*. The instrument of decrease of silver nanoparticles tried with the assistance of nitrate reductase test, which observed to be sure consequently, the writers reasoned that the NADPH subordinate nitrate reductase compound NADH oversees the diminishment of silver. The lessening of Ag+ particles by mixes of biomolecules found in these concentrates, for example, catalysts/proteins, amino acids, polysaccharides, and vitamins is ecologically kind, yet synthetically unpredictable. In any case, the system which is generally acknowledged for the combination of silver nanoparticles is the nearness of chemical "Nitrate reductase" (Mahendra *et al.,* 2009).

Nitrate reductase is a catalyst in the nitrogen cycle in charge of the transformation of nitrate to nitrite diminishment interceded by the nearness of the compound in the life form has been observed to oversee the blend. The utilization of a catalyst a-NADPH subordinate nitrate reductase in the in vitro combination of nanoparticles is imperative since this would get rid of the downstream handling required for the utilization of these nanoparticles in homogeneous catalysis and different applications, for example, nonlinear optics. Amid the catalysis, nitrate is changed over to nitrite, and an electron will be carried to the approaching silver particles (Duran *et al.,* 2005).

Albeit all these are the hypothesis, coordinate confirmation was given by Anil Kumar *et al.,* (2007) who specifically utilized the cleansed nitrate reductase from the creature *Fusarium oxysporum* for the union of silver nanoparticle in the test tube. Their response blend contained just the protein nitrate reductase, silver nitrate, and NADPH. Gradually, the response blend turned dark colored with every one of the attributes of silver nanoparticles. This is the principal coordinate proof for the association of nitrate reductase in the amalgamation of silver nanoparticles. And, Jain *et al.,* (2010) announced that the proteins in charge of the combination and soundness (topping operator) of silver nanoparticles utilizing the growth Aspergillus flavus with an atomic weight of 32 kDa might oversee the amalgamation and one of 35 kDa oversees the security of silver nanoparticles.

The silver particles shaped can be accomplished by measuring the XRD-range of the examples. X-beam diffraction jumped out at affirming the crystalline idea of the nano-molecule and the XRD design got has been spoken to in Figure (6). The XRD design indicated extreme crests in the entire range of 20 esteems running from 20 to 80. The XRD-range measured in most of the cases frequently parasitic concentrates brought about four exceptional pinnacles. The four serious pinnacles saw in the range consent to the Braggs' impression of silver nanocrystals detailed in the writing (Lu *et al.,* 2003). This further affirms the silver nanoparticles framed in the extracellular filtrate are available as silver nanocrystals, and, Shaligram *et al.,* (2009) who affirmed that X-beam diffraction design showed the crystalline structure of silver nanoparticles. In this way, the XRD range affirmed the nearness of silver nanoparticles. Silver nanoparticles from every contagious concentrate utilized have been described utilizing XRD by different specialists. The measure of silver nanoparticles can likewise be controlled by laser diffraction. Chosen zone electron diffraction (SAED) detects that compared to the (from inside to the outside of the focus ring) planes of the face-focused cubic (FCC) structure of natural silver are unmistakably found in Figure 5.

Additionally, thinks about were done utilizing Fourier Transform Infrared Spectroscopy. FT-IR is an intense apparatus for recognizing sorts of concoction bonds in an atom by delivering an infrared ingestion range that resembles a sub-atomic "unique mark". FT-IR spectroscopy is helpful for measuring optional structure in the metal nanoparticle protein connection by the ingestion of infra-red (IR) radiation through the reverberation of non-focus symmetric (IR dynamic) methods of vibration. The wavelength of light ingested is normal for the compound bond as can be found in this commented on the range. Since the quality of the assimilation is corresponding to the focus, FTIR can be utilized for quantitative investigations.

The FT-IR estimation can likewise be used to consider the nearness of a protein particle in the arrangement (Sastry *et al.,* 2003).

Presently, FTIR estimations of lyophilized nanoparticle tests were done after 24 h of brooding with the growth to recognize the conceivable biomolecules in charge of the lessening of the Ag+ Ions and topping off the bio-decreased AgNPs blended by parasitic filtrate. Agent spectra of acquired nanoparticles show assimilation tops situated at around 1045, 1245, 1299, 1361, 1377, 1488, 1550, and 1631 in the locale 1000– 1800 cm-1. The FTIR spectra uncover the nearness of various utilitarian gatherings like C–N, C– O– C, amide linkages, 1400 to1700 cm-1 district gives data about the nearness of "C=O" and "N-H" gatherings, these might be between amino corrosive deposits in polypeptides and protein in integrated silver nanoparticles and offer ascent to surely understood marks in the infrared area of the electromagnetic range (Table 10 and figure 8).

Prior FTIR examines were done to break down the nearness of proteins in the biosynthesized nanoparticles. It is accounted for that proteins can tie to nanoparticles. Either through free amine gatherings or cysteine deposits in the proteins and consequently potentially settle the silver nanoparticles. The plausible instrument for the nanoparticles biosynthesis and part of proteins amid the same has been accounted for by Ahmad *et al.,* (2003a). These reports proposed the plausible part of NADH-subordinate nitrate reductase in the decrease of the silver particle to metallic silver. The diminishment may happen by methods for the electrons from NADH where the NADH-subordinate reductase can go about as a bearer as per (Sastry *et al.,* 2003).

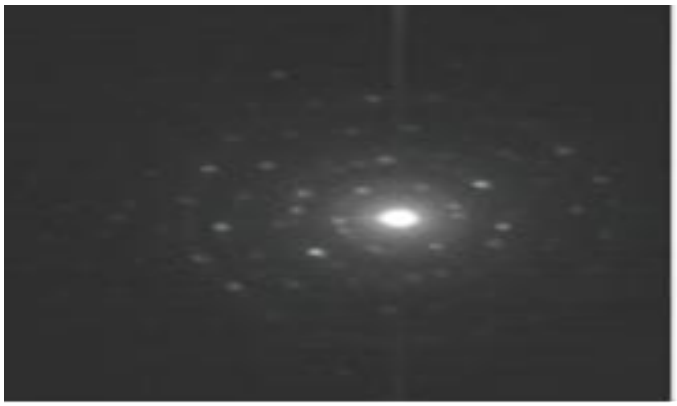

Fig. 5. Selected area electron X-ray diffraction showing the characteristic crystal planes of elemental silver from all fungal extracts used in the present study

Table 9. FTIR peaks and their respective assigned functional groups

FTIR peak (cm^{-1})	Assigned functional groups	FTIR peak (cm^{-1})	Assigned functional groups
1045	–C–O–C–	2900	CH2 n–
1245	Amide III	1485 and 1369	CH-
1350	C–N stretching vibrations of aromatic	1419	C=O
1388	Residual NO^{3-}	1720	N-H
1454	Symmetric stretching vibrations of –COO	3679	O-H stretching
1519	Amide II	3463	interlayered O-H stretching (H bonding)
1600	Aromatic C–C skeletal vibrations	1658 and 1542	H-O-H bending
1631	Stretch vibration of C=C	624	Al-OH
3358	the stretching vibrations of primary amines	2977, 1446, and 1326	–CH2 и–CH groups
2939	the stretching vibrations of secondary amines	1265–1288	—C–N bond
1423	C–N stretching vibrations of aromatic amines	3811	cm-1 (–NH group of amines
1029	C–N stretching vibrations of aliphatic amines	3463	(-OH group of phenols),
1651	primary amine NH band,	2012	aromatic –CH stretching
1554	secondary amine NH band	1631	-NHCO of amide
1423	methylene scissoring vibration from the protein in the solution	2920 and 2422	– COOH group in control cells

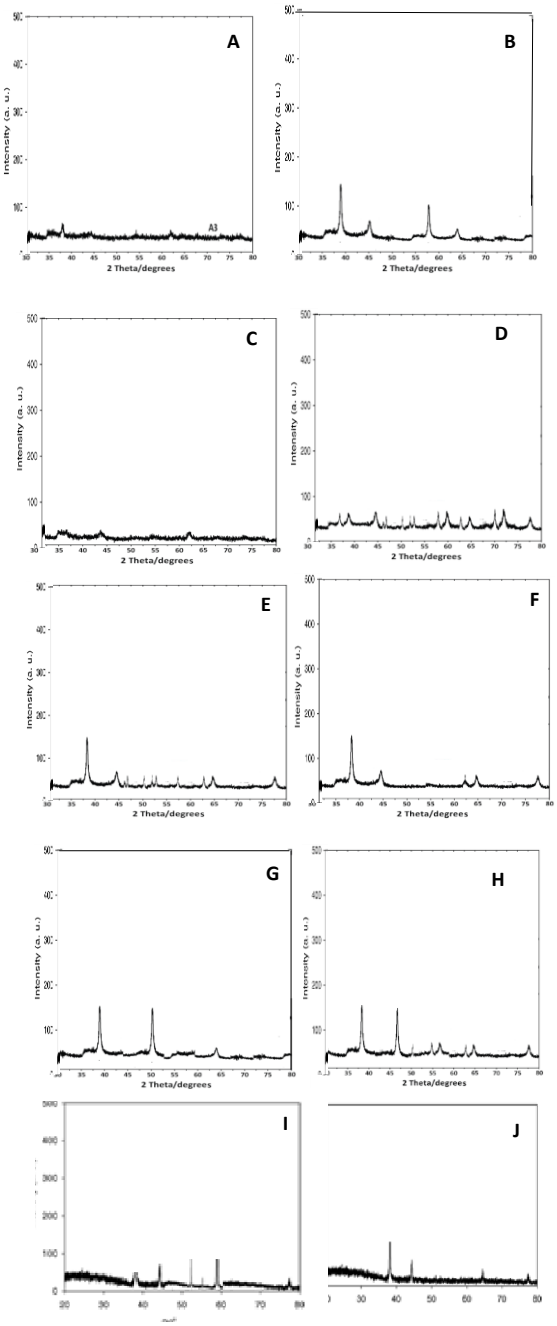

Fig. 6 X-ray diffraction (XRD)

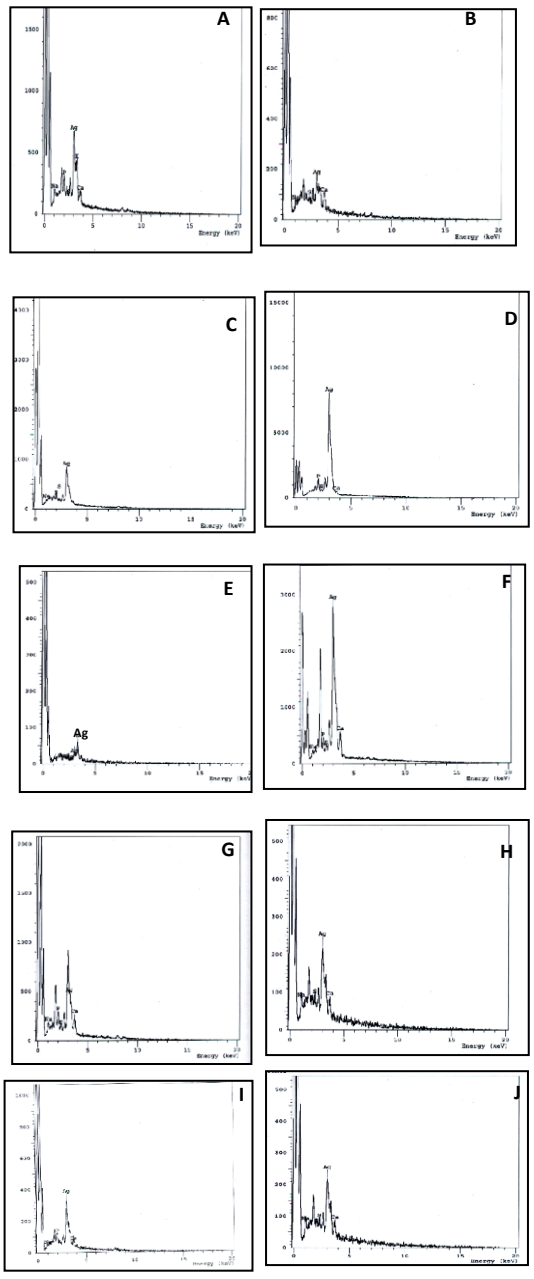

Fig. 7. Energy-dispersive X-ray spectrum (EDX)

Spectra of silver nanoparticles synthesized using fungal biomass (extra and intra cellular) after treated with silver nitrate (6 mM) solution and 72 h of incubation

(A): extracellular of *P. aurant.;* (B): intracellular of *P. aurant.*; (C): extracellular of *P. roquef.;* (D) : intracellular of *P. roquef.;* (E): intracellular of *A. niger.;* (F): intracellular of *V.chlamy.*; (G): extracellular of *T. viride;* (H) : intracellular of *T. viride;* (I): extracellular of *T. long.;* (J) : intracellular of *T. long.*

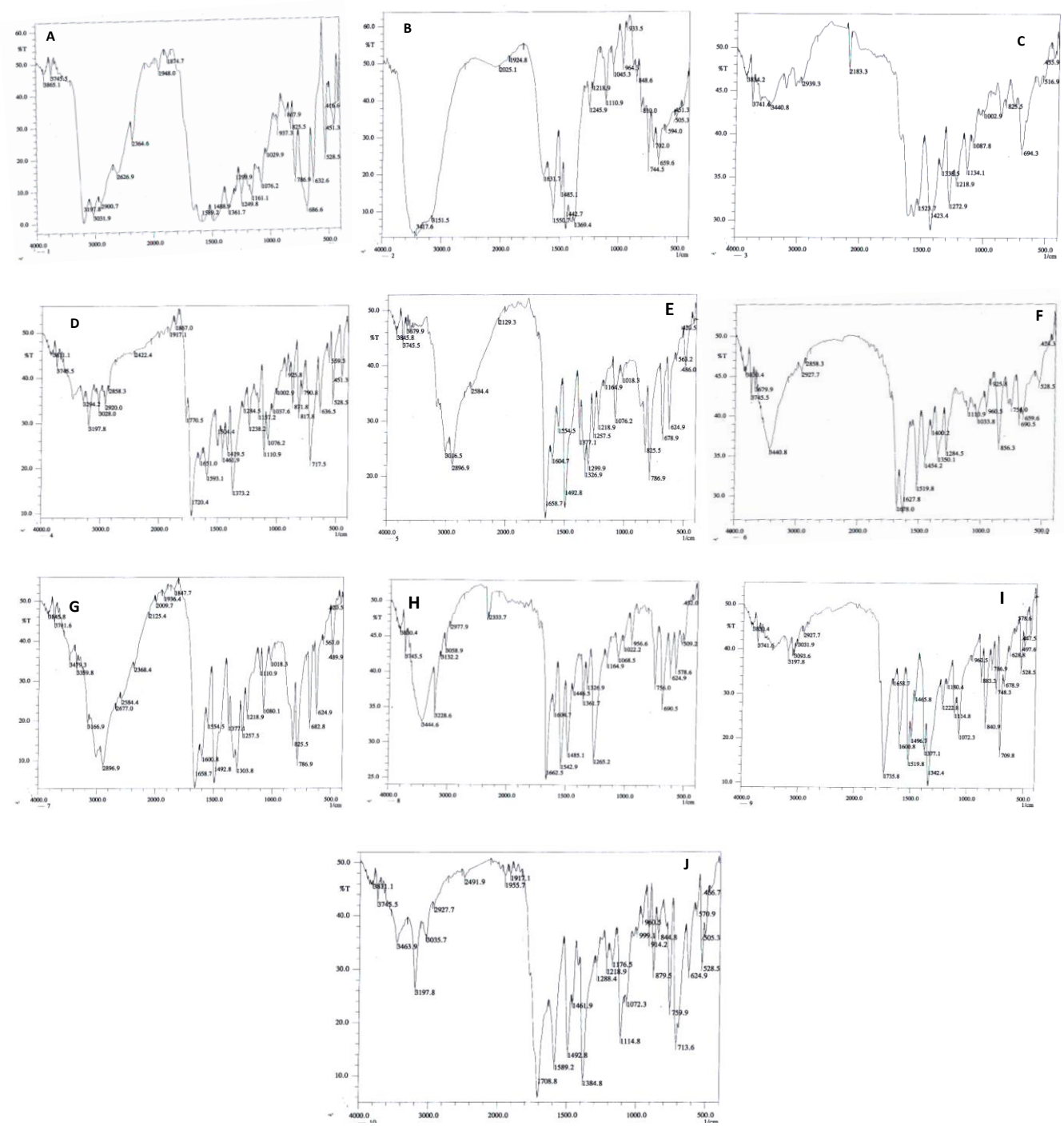

Fig. 8. FTIR spectra of silver nanoparticles synthesized using fungal biomass (extra and intra cellular) after treated with silver nitrate (6 mM) solution and 72 h of incubation
(A): extracellular of *P. aurant.;* (B): intracellular of *P. aurant.*; (C): extracellular of *P. roquef.;* (D) : intracellular of *P. roquef.;*
(E): intracellular of *A. niger.;* (F): intracellular of *V.chlamy.*; (G): extracellular of *T. viride;* (H) : intracellular of *T. viride;*
(I): extracellular of *T. iona.;* (J) : intracellular of *T. iona.:*

Accordingly, in a similar study per Sharmila et al. (2018), the AgNPs were orchestrated at room temperature utilizing *P. guajava* leaf separate. The plant phytochemicals particles are in charge of the lessening of AgNPs and improved antibacterial action. FTIR investigation underpins the nearness of practical gatherings of biomolecules topped on the arranged AgNPs. These green courses blended AgNPs were preparatory recognized by visual investigation where the adjustment in shading was confirm, and after that diverse portrayal methods were executed to demonstrate the nearness of AgNPs. The retention range and XRD considers confirm the nearness of AgNPs. Electron magnifying instrument strategy, for example, FESEM and TEM examination affirmed the circular shape and size of about ~55 nm of the un-agglomerated AgNPs. The natural examination likewise affirms the nearness of Ag in the readied test. The antibacterial movement of AgNPs was done against *E. coli* and *S. aureus* and its zone of hindrance was measurement subordinate way. Also, the present examination showed quick, eco-accommodating, practical and essentially course to incorporate AgNPs from *biological route* benefits for biomedical applications.

Vitality dispersive X-beam range (EDX) examination demonstrates the crest in silver district affirming the nearness of natural silver. The optical retention top is watched roughly at 3 keV, which is run of the mill for the assimilation of metallic silver nanocrystalline because of surface plasmon reverberation, from this we affirmed the nearness of nanocrystalline natural silver (Figure 7). The nearness of solid signs predictable with basic silver together with feeble signs from Na, P, S, K, Ca, Cu, Cl and Fe molecules are seen in the EDX investigation of the orchestrated nanoparticles (Table 9). The C, N, and O signs may emerge from proteins, compounds, or the parasitic biomass which are bound or close to the silver nanoparticles. The Cl flag demonstrates the nearness of a little sum, Na, P, and Ca signals are likely caused by X-beam discharge from the glass substrate utilized as a part of the EDX examination (Mohammed *et al.,* 2009).

CONCLUSION

Decisively, it has been exhibited that numerous filamentous contagious species have demonstrated the potential for the additional and intra-cell combination of decently monodispersed silver nanoparticles (AgNPs) in the scope of 8.17– 16.73 nm. The energy connected through this examination of silver nanoparticles blend utilizing contagious sans cell filtrate demonstrates a fast combination of nanoparticles that would be reasonable for building up a natural procedure for mass scale generation industry. This procedure was advanced controlled by pH, temperature, silver substrate focusses and introduction time to silver nitrate. The created AgNPs are very steady in the arrangement because of the topping of silver nanoparticles by proteins emitted by the growth. Moreover, the additional and intracellular combination would make the procedure more straightforward and less demanding for downstream preparing. In future, it is vital to comprehend the biochemical and sub-atomic component of the blend of the nanoparticles by the cell filtrate with a specific end goal to accomplish better control over size and polydispersity of the nanoparticles. The biosynthesis of nanoparticles must get more consideration because of the developing need to create safe, financially savvy and earth agreeable advancements for nanomaterial's union. The ebb and flow inquire about to open another road for the green combination of nonmaterial.

ACKNOWLEDGEMENT

The authors might want to express extraordinary because of staff individuals from the Regional Center for Mycology and Biotechnology (RCMB), Al-Azhar University, Cairo, Egypt, for endeavors applied at the research facility tests, chemicals utilized and in addition the explored microbial species along this work. They likewise might want to acquaint an incredible gratefulness with staff individuals from the Ain Shams University Genetic Engineering (ASUGEN) consider administrations unit, Cairo, Egypt for aiding in protein SDS-PAGE, decontamination, and electrophoresis through this examination.

CONFLICT OF INTEREST

There is no conflict of interest.

REFERENCES

Ahmad, B., Mukherjee, S., Sastry, M., 2003[a]. Extracellular biosynthesis of silver nanoparticles using the fungus *Fusarium oxysporum*, Colloids Surf. B 28 : 313–318.

Ahmad, A., Senapati, M., Sastry, M., 2003[b]. Extracellular biosynthesis of monodispersed gold nanoparticles by a novel extermophillic actinomycete, *Thermonospora* sp., Langmuir 19: 3550–3553.

Akinsiku, A.A., Enock, O.D., Kolawole, O.A., Joseph A.A., Joan, A.A., 2018. Green Synthesized Optically Active Organically Capped Silver Nanoparticles using Stem Extract of African Cucumber (Momordica charantia). J. Mater. Environ. Sci., JMES, 9(3): 902-908.

Anil Kumar, S., Abyaneh, M., Ahmad, A., Khan, M.I., 2007. Nitrate reductase mediated synthesis of silver nanoparticles from $AgNO_3$. Biotechnol Lett., 29:439–445.

Banerjee, A., Theron, R., Scott, R.W., 2014. Redispersion of sinthered nanoparticles catalysts in tetra alkylphosphonium ionic liquid. J. Mol. Catal. Chem., 393:105-11.

Bharde, A., Rautaray, D., Bansal, V., Sanyal, M., Sastry, M., 2006. Extracellular biosynthesis of magnetite using fungi. Small 2: 135–141.

Cohen, M.S., Stern, J.M., Libertino, J.A., 2007. *In vitro* analysis of a nanocrystalline silvercoated surgical mesh. Surg. Infect. 8: 397–403.

Duran, N., Marcato, P., Esposito, E., 2005. Mechanistic aspects of biosynthesis of silver nanoparticles by several *Fusarium oxysporum* strains. J. Nanobiotech., 3:8–14.

Elliott, C., 2010. The effects of silver dressings on chronic and burns wound healing. Br. J. Nurs., 19: 32–36.

Hames, B.O., Rickwood, D. 1990. Gel Electrophoresis of Proteins, a Practical Approach" (2nd Ed.) Oxford University Press, USA,; pp. 1-147.

Hayat, M.A., 1990. Colloidal Gold: Principles, Methods and Applications, Academic Press, San Diego, CA, 1990.

Jain, N., Bhargava, A., Majumdar, S. and Panwar, 2010. Extracellular biosynthesis and characterization of silver nanoparticles using *Aspergillus flavus* NJP08: A mechanism perspective. The Royal Society of Chemistry 70-79.

Kathiresan, K., Manivannan, M.A. and Nabeel, B., 2009. Studies on silver nanoparticles synthesized by a marine fungus, *Penicillium fellutanum* isolated from coastal mangrove sediment. Colloids and Surfaces B: Biointerfaces 71: 133–137.

Kilin, D.S., Prezhdo O.V., Xia, Y., 2008. Shape-controlled synthesis of silver nanoparticles: Ab initio study of preferential surface coordination with citric acid. Chem. Phys. Lett., 6: 113–116.

Kuber, C., Bhainsa, S.F., Souza, D., 2006. Extracellular biosynthesis of silver nanoparticles using the fungus *Aspergillus fumigatus* Colloids and Surfaces B: Biointerfaces 47: 160–164

Li, Y., Duan, X., Qian, Y., Liao, H., 1999. Nanocrystalline silver particles: synthesis, agglomeration, and sputtering induced by electron beam. J. Colloid Interface Sci., 209:347-349.

Lowry, O., Rosebrough, A. L., Randall, J., 1951. Protein measurement with the Folin phenol reagent. J. Biol. Chem., 193:265-275.

Lu, H.W., Liu, S.H., Jhu, J.K., 2003. Silver nanocrystals by hyperbranched polyurethane-assisted photochemical reduction of Ag^{+}, Mater. Chem. Phys., 81: 104–107.

Mahendra, R., Alka, Y., Gade, A., 2009. Silver nanoparticles as a new generation of antimicrobials. Biotechnol. Adv., 27: 76–83.

Marcato, P.D., Duran, N., 2008. New aspects of nanopharmaceutical delivery systems. J. Nanosci. Nanotechnol., 8: 2216-2229.

Mohammed, F., Balaji, P., Venkatesanc, R., 2009. Fungal based synthesis of silver nanoparticles—An effect of temperature on the size of particles. Colloids and Surfaces B: Biointerfaces 74: 123–126.

Nia, P.M., Meng, W.P., Alias, Y., 2015. Hydrogen peroxide sensor: Uniformly decorated silver nanoparticles on polypyrrole for wide detection range. App. Surf. Sci., 357: 1565-72.

Sastry, M., Ahmad, A., Khan, M., 2003. Biosynthesis of metal nanoparticles using fungi and actinomycete. Current Sci., 85:162–170.

Shaligram, N.S., Mahesh, B., Singhal, S., 2009. Biosynthesis of silver nanoparticles using aqueous extract from the compactin producing fungal strain. Process Biochem., 44: 939 – 943.

Sharmila, C., Ranjith K.R., Chandar, S.B., 2018. Psidium guajava: a novel plant in the synthesis of silver nanoparticles for biomedical applications. Asian J. Pharm. Clin. Res., 11(1): 341-345.

Singh, R., Singh, N.H., 2011. Medical applications of nanoparticles in biological imaging, cell labeling, antimicrobial agents, and anticancer nanodrugs. J. Biomed. Nanotechnol., 7:489-503.

Solomon, M.M., Umoren, S.A., 2016. In-situ preparation, characterization and anticorrosion property of polypropylene glycol/silver nanoparticles composite for mild steel corrosion in acid solution. J. Colloid Interface Sci., 462:29-41.

Sriram, M. I., Selvaraj, B.K., Kalimuthu, K., 2010. Antitumor activity of silver nanoparticles in Dalton's lymphoma ascites tumor model. Int. J. Nanomed., 5: 753–762.

Tripathy, A., Ashok, M., Raichur, N., Chandrasekaran, T., Prathna A., 2010. Process variables in biomimetic synthesis of silver nanoparticles by aqueous extract of *Azadirachta indica* (Neem) leaves.Nanopart. Res., 12:237–246.

Zhao, G.J., Stevens, S.E., 1998. Multiple parameters for the comprehensive evaluation of the susceptibility of *Escherichia coli* to the silver ion. Biometals, 11: 27–32.